Analysis and Design of Long Span Deep Corrugated Structural Plate Bridges in High Seismic Zones

M. Meckkey El-Sharnouby

Principal Engineer, PhD, P.Eng., PE (NV)

Atlantic Industries Limited

Adjunct Professor (Western University)

Cambridge, ON

melsharnouby@ail.ca

Hany El Naggar

Professor, PhD, P.Eng.

Dalhousie University

Halifax, NS

Hany.Elnaggar@dal.ca

Paper prepared for the session Transportation Infrastructure

2025 Transportation Association of Canada (TAC) Conference & Exhibition

Québec City, Québec

Abstract

Long-span, deep-corrugated structural plate bridges have proven effective over the past three decades, with spans reaching up to 32.4 m. While seismic analysis of these structures has historically relied on simplified methods across all seismic zones, CSA S6-19 and S6-25 introduced more rigorous requirements for high seismic zones, including the racking method and non-linear time history analysis. This paper explains and investigates two approaches for estimating the crucial shear displacement profile needed for racking analysis. The seismic performance of the largest such bridge in Canada is examined, assuming a site in Montreal, a region of high seismic hazard. The findings indicate that for the conditions considered, a commonly employed semi-empirical method yields a shear displacement profile consistent with 1D ground response analysis. Furthermore, the soil profile, particularly the bedrock elevation, significantly influences the predicted shear displacement. Finally, the study underscores the importance of carefully considering the relative location of the shear displacement load profile with respect to the bridge structure when applying the racking method.

Introduction

Metal corrugated structures have been in use for infrastructure applications for over a century. Corrugated steel pipes (CSP) were invented for use for culverts in 1896. With manufacturing and technological evolutions, diameters reached 3000 mm or larger. In 1931, To accommodate heavier loads and larger spans, structural plates with shallow corrugations were developed. A few decades later, deep corrugated structural plates were developed. These structures are assembled on-site by bolting corrugated plates together to form "rings." `The largest structural plate bridge, known as, steel buried bridge or structure spans 32.4 m, and is located in United Arab Emirates. The largest metal bridge in Canada is located in St. John's, NL and spans 25.4 m. The performance of long span deep corrugated plate bridges under static loading has been investigated by several authors including, Brachman et al. (2013) Embaby et al. (2021, 2022and 2023). Seismic performance, however, has received limited attention.

Seismic hazard in Canada has considerably increased over the past two decades. The higher probability of exceedance of strong ground motions pauses a higher risk on life safety and on Canadian infrastructure. As buried structures are contained by surrounding soils, seismic performance records have been favourable when compared to other bridge types (NCHRP 611). Under seismic loading, ovaling and/or and racking deformations may be caused by vertically, horizontally, or obliquely propagating seismic waves of any type. Wang (1993) provided a pseudostatic analysis approach for cut-and-cover small span buried structures which was later adopted in NCHRP 611 (2011) and FHWA (2011). Byrne et al. (1996) investigated the performance of buried steel and concrete structures under seismic loading using pseudostatic and two-dimensional time history analysis methods. The investigation considered horizontal and vertical motions with PGA of 0.2g and PGA of 0.13g, where PGA is the peak vertical ground acceleration. The study indicated that increase in the seismic induced thrust is due to the vertical motion while the increase in the seismic induced moment is due to the horizontal motion. Relative to the time history analysis, the pseudostatic was found to be conservative in predicting thrust and appropriate for predicting moment. Mahgoub and El Naggar (2021) investigate the performance of 9.5 m span deep-corrugated bridge in high seismic zones using non-linear time history analysis. They

found that commonly adopted simplified equations may not be appropriate for structures in seismic zone. This study focuses on investigating the two common methods for estimating the shear displacement profile resulting from vertically propagating shear waves. The shear displacement profile is used to predict the seismic demand on an example buried structure, which is the so-called method, racking approach. The racking method is one of the methods included in the CSA S6-25 commentary update.

Current provisions in CSA S6-19 and 25

Design methods for bridges are regularly evolving to provide safe and economical solutions to the increased seismic hazard. In the CSA S6-19, the seismic provisions for buried structures were updated. Seismic zones are implicitly categorized as low and high seismic zones. The criteria for the seismic category is the spectral acceleration of the subject site at 2% probiality in 50 years. For low seismic zone, the simplified method that existed in the previous versions of the standard is permitted. The earthquake effects are determined primarily by the peak ground acceleration of 2% at 50 years, PGA, as shown in Eq. 1.

$$T_E = 2/3 \times PGA \times T_D \quad \text{Eq 1}$$

$$M_E = 2/3 \times PGA \times M_D \quad \text{Eq 2}$$

Where, TE and TD are seismic induced thrust and dead load thrust, and ME and MD are seismic induced bending moment and dead load bending moment, respectively.

Mahgoub and El Naggar (2019) compared the structure internal forces estimated from the simplified method to two-dimensional non-linear time history analysis. They found that for high seismic zones, the simplified method underestimates the structure internal forces, and that full dynamic analysis is required. CSA S6-25 Commentary provides further information on the types of detailed analysis required depending on bridge classification, critical, major or other, and soil class. The two methods of analyses are full shaking analysis and the racking method. However, additional guidance may be needed on applying these analysis techniques to buried structures.

Semi-empirical procedures

Anderson et al. (2008) in their NCHRP 611 report, seismic analysis and design of retaining walls, buried structures, slopes and embankments, presented a deformation-based approach for determining the straining actions on buried structures. The study focused on close-bottom round structures up to 3.048m in diameter and box structures up to 6.1m in span. Closed form solution predicting the maximum induced racking displacement in the structure were compared with pseudo-accelerations of 0.3g for a range of soil cover heights, and soil and structure properties. The seismic induced straining actions were estimated based on vertically propagating horizontal shear waves, i.e., vertical motions were not considered. FHWA (2011) stated that vertical ground strains are much smaller than shearing strains because the confined modulus of compressibility is much larger than the soil shear modulus. The report presented an alternative approach to determine the racking displacement. The maximum induced shear stress is estimated from Seed and Edris (1971) simplified approach as,

$$\tau_{max} = (PGA / g)\, \sigma_v . R_d \quad \text{Eq 3}$$

where,

σ_v is the total overburden pressure, and R_d is a stress dependant reduction factor. The maximum induced shear strain, γmax, can then be calculated from τ_{max} and the strain compatible shear modulus, G_m as shown in Equations 4.

$$\gamma_{max} = \tau_{max} / G_m \quad \text{Eq 4}$$

$$\Delta_{free\ field} = \gamma_{max} . H \quad \text{Eq 5}$$

Seed and Edriss (1971) provided curves for R_d versus depth that shows significant variability for depths below 20 m. FHWA (2011) provided back calculated formulas for depths up to 30 m (100 feet) representing the average of the values presented by Seed and Edriss (1971), with a min value of 0.5 for depths more than 100 feet. Katzenbach et al. (2013) presented the latest developments in estimating Rd and found that additional research may be needed. Figure 1 shows the variation of free field displacement for an earthquake with PGA of 1g with R_d based on FHWA (2011), the lower bound of data presented by Seed and Edris (1971), and R_d equal to unity. The curves show that the FHWA (2011) method predicts free-field displacements that is approximately 35% of the lower bound method along the top 10 m. Buried structures with spans up to 20 m would be within the upper 10 m below the ground elevation. When semi-empirical method presented in Eq 3 and Eq 4 is used solely to predict the free-field displacement, consideration of sensitivity of structure response to the variation of Rd is recommended.

Figure 1. Free-field displacement for Rd based on FHWA 2011, lower bound (Seed and Idriss, 1971) and $R_d = 1$

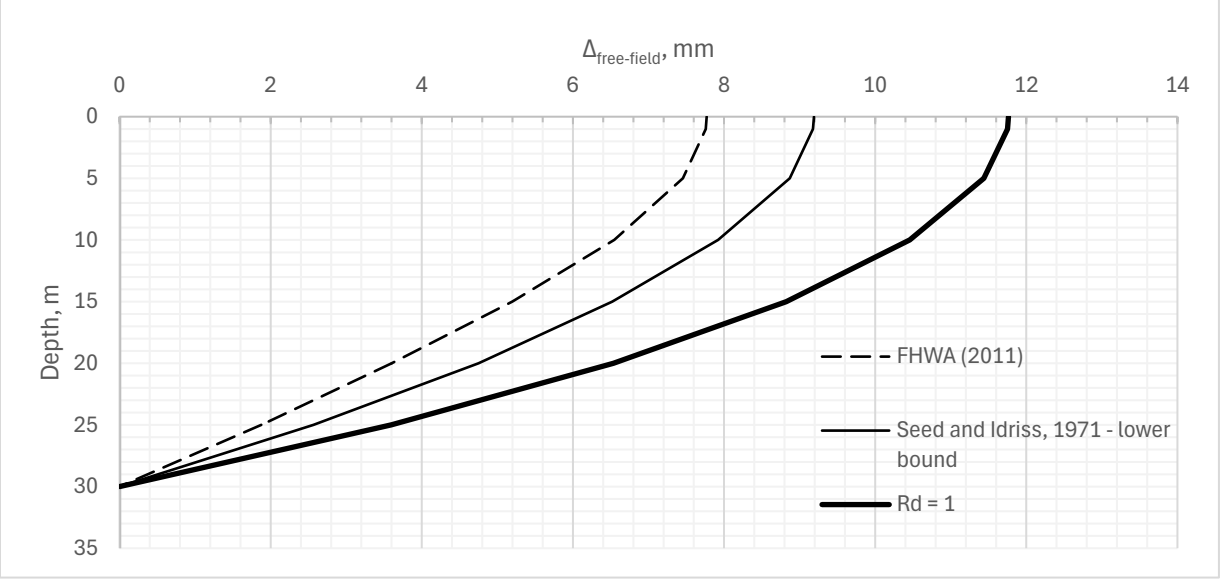

Free field displacement profile for an example profile in Montreal

Equations 3 and 4 show that free field displacement depend in the PGA and the soil stiffness. The PGA is for 2% probability of exceedance in 50 years or 1: 2500. PGA values is dependant on location of the

subject site and the average shear wave velocity in the top 30 m of soil, as per CSA S6-19. The reader is referred to the aforementioned standard for additional conditions for determining the site classification. Structure backfill are typically placed adjacent to the structure at a minimum width as specified by CSA S6-19. Embankment fill is placed beyond the backfill zone which in most cases has lower stiffness and strength characterises than structural backfill. As such, soil profile from bottom of footing or pile cap to road grade should be considered for site classification, in addition to the 30 m below the bottom of the footing. The shear displacement profile is then a function of the depth of bedrock. i.e, sites where bedrock is found at lower elevation will exhibit higher shear displacements compared to sites with high bedrock elevation.

Depth of bedrock varies across Montreal depending on the site location. Three soil profiles below the footings elevation are assumed. Seismic and soil parameters associated with the three soil profiles are presented in Table 1, and the resulting free-field displacements are shown in Figure 2. For soil profile I, the site classification is C as backfill material is assumed from bottom of footing to road grade while for soil profile II and III, 20 m of soil Class C and D are assumed, respectively. As can be seen from Soil profile I and II which have the same site class, the depth of bedrock can substantially influence the predicted free field displacement. Soil profile III which is designated as site class D with 30 m of soft soil resulted in free field displacements that are 200 % more than that of Soil Profile II. These example calculations show that the calculation method for estimating the shear displacement from the maximum shear stress presented in Anderson et al. (2011) and FHWA (2011) should be modified and integration of the shear strain displacement profile to obtain the settlement profile is recommended.

Examining Soil Profile II and III, the influence of site class and the strain compatible shear modulus can also be realized. G_m values depend on soil type, grain size distribution, unit weight, shear wave velocity, and ratio of shear modulus at actual strain level to maximum shear modulus. It is recommended that a reasonable bandwidth of G_m values be established rather than utilizing one deterministic value.

Table 1. Soil profiles and PGA considered for example calculation of $\Delta_{\text{free field}}$

Soil profile	**I**	**II**	**III**
Competent soil	20 m	0 m	0 m
Very dense soil	0 m	20 m	0 m
Bedrock	30+ m	30+ m	below footings
Backfill around structure	Yes	Yes	Yes
Bottom of footing to road elev.	10 m	10 m	10 m
Site Class	D	C	C
PGA (g)	0.421	0.48	0.48
G_m (MPa)	11765	41176	41176

Figure 2. Free field displacement for soil profiles considered for Montreal.

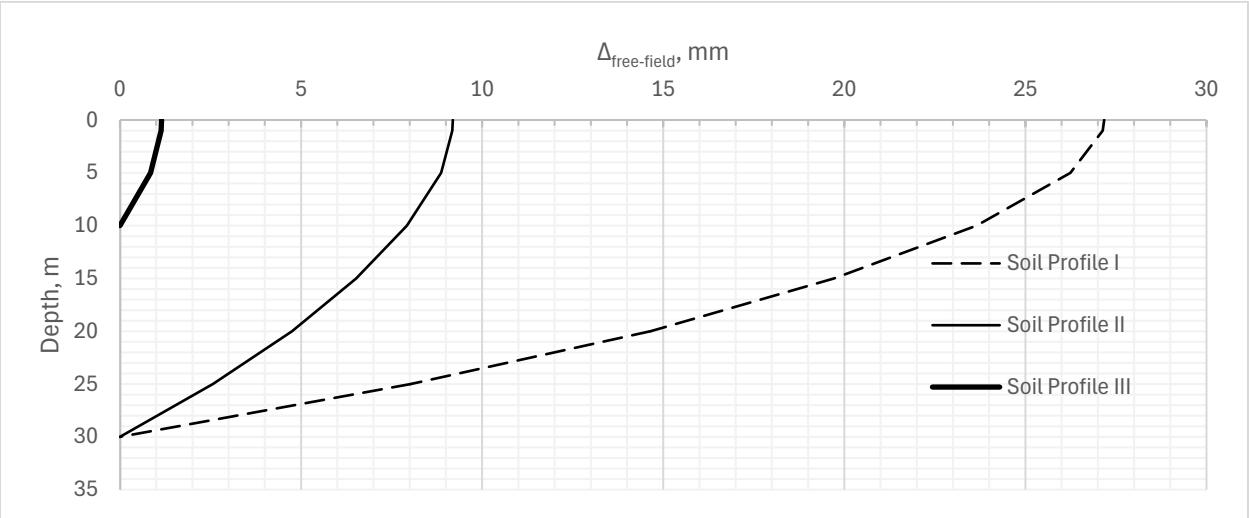

Free Field Site Response Analysis with 1-D FE Modelling

The site location selected for this paper is Montreal. CSA S6-19 requires selection of minimum of 11 records amongst other criteria when conducting site response analyses. With the purpose of this paper to provide an insight into prediction of free-field displacement using the semi-empirical approach and the 1D site response analysis, one records was selected representing M6 earthquake. The records are part of the library of records provided by Atkinson [2009}. The record, as shown in Figure 3, was scaled to match the NBCC 2020 spectral acceleration for 2% in 50 years probability of exceedance for site classification C. For clarity the record is shown from time of 19 seconds to 23 seconds. Spectral acceleration for the scaled record is plotted against the target spectral acceleration in Figure 4.

Figure 3. M6 Earthquake record selected for 1D site response analysis (before scaling).

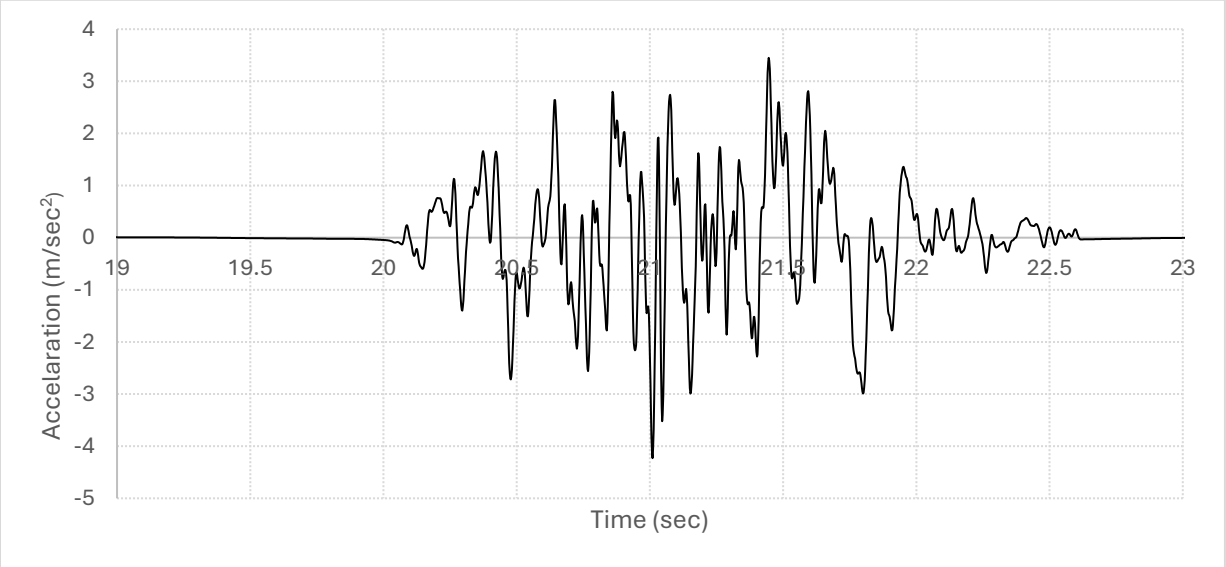

Figure 4. Target and simulated spectral acceleration for Site Class C in Montreal (Vs_{30} = 300 m/sec)

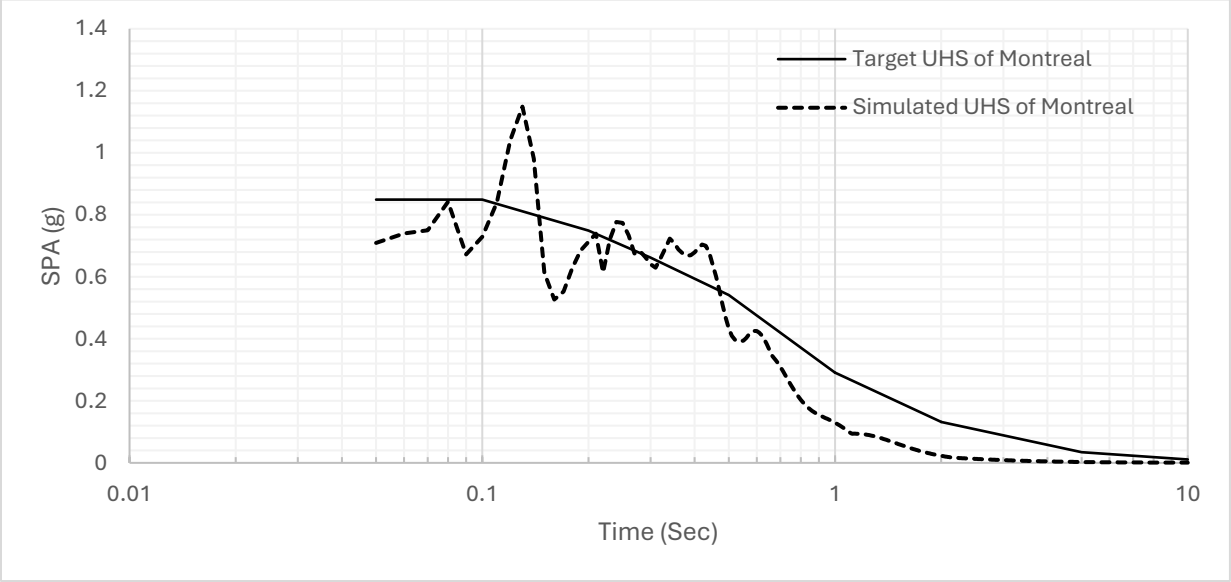

The soil profile selected is Soil Profile II shown in Table 1. The model geometry consisted of 30 m of very homogeneous soil that was modelled using 15-node triangular elements. The material model is a non-linear strain hardening model developed by Benz (2006). The model parameters are shown in Table 2.

Table 2. Soil properties for 1D FE site response analysis

Material	E, Mpa	E_{oed}, MPa	E_{ur}, MPa	Unit weight, kN/m^3	Peak friction angle
Dense sand	70	72	210	22	40

Figure 5 shows the results of the 1D FE site response analysis. For comparison purposes, the semi-empirical method predictions are plotted. The maximum displacement at top of road grade predicted by the semi-empirical method is consistent with the 1D site response analysis. The semi-empirical method utilizing the stress dependant reduction factor by the lower bound of Seed and and Idriss (1971) is slightly conservative while the FHWA (2011) values may be unconservative.

Figure 5. Shear displacement profile from site response analysis and semi-empirical method

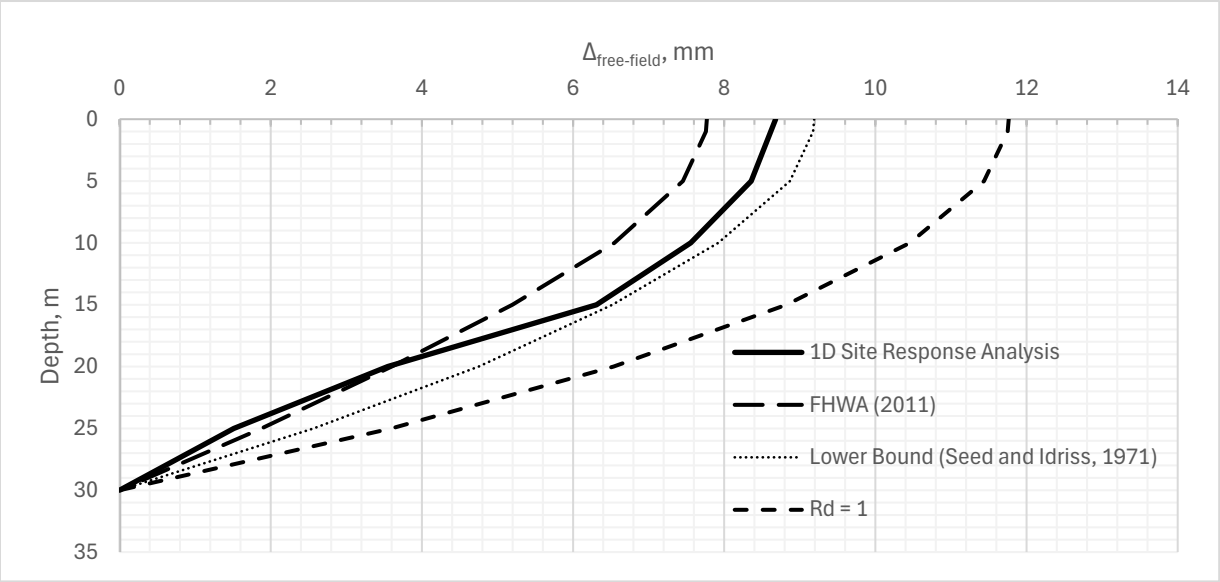

Seismic Demand on deep corrugated structural plate bridges

Buried structures subjected to vertically propagating shear wave can be evaluated using non-linear time history analysis as demonstrated by Mahgoub and El Naggar (2021). Alternatively, seismic demand can be evaluated by the racking method consisting of applying the shear displacement along the soil profile in two-dimensional numerical model. CSA S6-25 commentary provides updated criteria for the appropriate seismic method based on the bridge category designation. As mentioned before, additional seismic analysis is required for all sites with spectral acceleration of 0.2 seconds at 2% in 50 years larger than 0.7 g is required. For lifeline bridges, non-linear time history analysis is required for Critical Bridges. For Major Routes and Other bridges, either method is permitted.

In this paper, the largest span structural plate bridge in Canada is considered for this example study. Site classification is assumed to be C and soil profile is assumed to be Profile II as shown in Table 2. The structure has a span of 25.4m and a rise of 6.4m. Fill height measures from top of footing to road grade is taken as 10 m. Well graded gravelly sand compacted to 98% standard proctor density is used as backfill and embankment soil.. The structure geometry and corrugation profile are shown below in Figures 6 and 7, as per CSA G401 (2024) and ASTM 796/796M (2018).

Figure 6. Structure geometry considered in this study

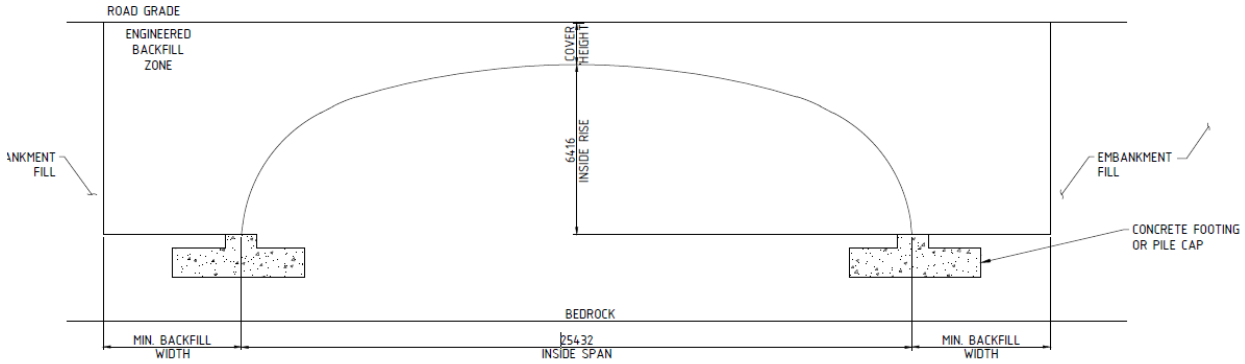

Figure 7. Corrugation profile for structure considered in this study

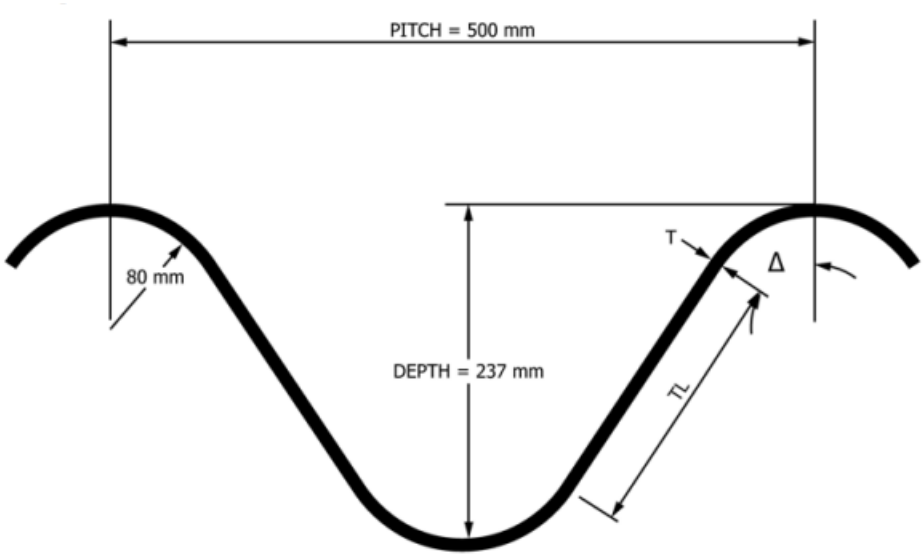

Two-dimensional finite element model is employed to simulate the soil-structure interaction. The structure is modelled as plate elements with properties as per ASTM 796/796M (2023). Backfill is modelled as two-dimensional 6-noded triangular elements. Material and geometric non-linearity are considered. The material properties are conservatively taken as those provided in Table 2. Placement of the backfill is simulated by placing backfill with a maximum differential of 0.5 m across the structure span. This approach tracks the evolution of soil and structure stresses throughout the construction phase.

The seismic forces are then applied as displacement on both sides of the structure, extending to the road grade so that the impact of the overburden pressure and interface of the soil above the structure is considered. Literature review by the authors of the references mentioned in this paper revealed that there is little guidance on location of the shear displacement across the width of backfill. To investigate the sensitivity of structure response to location of applied horizontal displacement, the displacement profile varied at 1, 2, 5 and 10 m. Table 3 provides the displacement, thrust and bending response of the structure relative to load positioned at 1 m away from the structure tip. The substantial decrease in

structural response compared to the 1 m load position highlights the critical importance of considering various load positions in racking analysis and assessing the sensitivity of the structure response.

Non-linear time history analysis offers a potential method for evaluating the representative position of the racking displacement. Although this approach is comprehensive and computationally demanding, it effectively captures the dynamic soil-structure interaction. Additionally, it allows for the analysis of how structure stresses evolve under seismic excitation.

Table 3. Variation of structure racking displacement with location of hor. disp. load

Distance from structure tip	1 m (reference)	2 m	5 m	10 m
Structure racking horizontal displacement*	1	0.73	0.18	0.04
Structure seismic thrust*	1	0.820	0.344	0.053
Structure seismic bending moment*	1	0.73	0.07	0.07

*relative to 1 m distance

Design Load Cases

As previously discussed, the simplified method in CSA S6-19 and S6-25 determines seismic thrust and bending moment as two-thirds of the peak ground acceleration multiplied by the dead load effects. While this approach's origin may trace back to Byrne et al. (1996), their research indicated that seismic thrust demand is proportional to half the peak vertical acceleration. The CSA S6-19 and S6-25 methods inherently suggest that the seismic demand corresponds to vertically propagating P-waves (compression waves). For the seismic ultimate limit state (ULS) design case, factored dead loads are combined with seismic loads using a load factor of 1.0 for the latter. In high seismic zones, where the horizontal effects need to be considered, the CSA S6-25 commentary stipulates consideration of four load cases: 1) dead load with vertical acceleration effects, 2) dead load with horizontal acceleration effects, 3) dead load with combined full vertical and one-third horizontal acceleration effects, and 4) dead load with combined one-third vertical and full horizontal acceleration effects. It's important to note that vertical acceleration effects predicted by the simplified method may be overly conservative. Furthermore, designing buried bridges for a 2% in 50-year event represents a more stringent criterion than that for Major or other Routes in CSA S6-25. To provide a more appropriate assessment of seismic demand, performance-based design of buried bridges is currently under investigation by the authors.

Conclusions

This paper examines the seismic performance of a long-span, deep-corrugated structural plate bridge located in Montreal, a region with high seismic hazard, using the racking analysis method as mandated by CSA S6-19 and S6-25. To determine the shear displacement profile for vertically propagating shear waves, two methodologies are presented: a semi-empirical approach and the racking method itself. Based on the results of this study, the following conclusions are drawn:

- Site classification for buried structures with backfill soils typically falls into Categories C, D, E, or F, depending on the soil properties beneath the structure's base, rather than Categories A or B.
- Establishing the shear displacement profile necessitates knowledge of the bedrock elevation.
- The strain-compatible shear modulus should be determined using a reasonable range of shear wave velocities.
- Shear displacement profile should be established by integration of the shear strain profile rather than using the depth of the soil layer from the ground surface.
- The shear displacement profile derived from the semi-empirical method aligns with the results of one-dimensional ground response analysis.
- Careful attention must be paid to the variation of the stress-dependent reduction factor with depth.
- The influence of the shear displacement profile's location relative to the bridge structure warrants further investigation.

References

ASTM A796/A796M-23, Standard Specification for Structural Design of Corrugated Steel Pipe, Pipe-Arches, and Arches for Culverts, Sewers, and Other Buried Applications, ASTM International, West Conshohocken, PA, 2023, www.astm.org.

Anderson, D. G., Martin, G. R., Lam, I., & Wang, J. N. (2008). *Seismic Analysis and Design of Retaining Walls, Buried Structures, Slopes, and Embankments* (NCHRP Report 611). Transportation Research Board, National Research Council, Washington, D.C.

Atkinson, G. M. (2009). Earthquake time histories compatible with the 2005 National Building Code of Canada uniform hazard spectrum. *Canadian Journal of Civil Engineering*, *36*(6), 991-1000.

Brachman, R. W. I., Elshimi, T. M., Mak, A. C., & Moore, I. D. (2012). Testing and Analysis of a Deep-Corrugated Large-Span Box Culvert Prior to Burial. *Journal of Bridge Engineering*, *17*(1), 81-88.

Byrne, P. M., Anderson, D. L., & Jitno, H. (1996). Seismic analysis of large buried culvert structures. *Transportation Research Record: Journal of the Transportation Research Board*, *1541*(1), 133-139.

Canadian Standards Association. (2019). *Canadian Highway Bridge Design Code* (CSA Standard No. S6-19).

Canadian Standard Association. (2019). *CSA S6.1:19, Commentary on CAN/CSA S6:19, Canadian Highway Bridge Design Code*. Mississauga, ON, Canada: CSA Group.

Choi, D.-H., Kim, G.-N., & Byrne, P. M. (2004). Evaluation of moment equation in the 2000 Canadian highway bridge design code for soil–metal arch structures. *Canadian Journal of Civil Engineering*, *31*(2), 281–291. https://doi.org/10.1139/l03-097

Clauss, F., Katzenbach, R., & Rochee, S. (2013). Recent developments in procedures for estimation of liquefaction potential of soils. In *18th International Conference on Soil Mechanics and Geotechnical Engineering* (pp. 1515-1518). Paris: ISSMGE

Embaby, K., El Naggar, M. H., & El-Sharnouby, M. (2023). Ultimate capacity of large-span soil-steel structures. *Tunnelling and Underground Space Technology*, *132*, 104887.

Embaby, K., El Naggar, M. H., & El-Sharnouby, M. (2022). Performance of large-span arched soil–steel structures under soil loading. *Thin-Walled Structures*, *172*, 108884.

Embaby, K., El Naggar, M. H., & El-Sharnouby, M. (2021). Response Evaluation of Large-Span Ultradeep Soil–Steel Bridges to Truck Loading. *International Journal of Geomechanics*, *21*(10), 04021150.

Federal Highway Administration, National Highway Institute. (2011). *LRFD Seismic Analysis and Design of Transportation Geotechnical Features and Structural Foundations Reference Manual* (FHWA-NHI-11-032). U.S. Department of Transportation, Federal Highway Administration.

National Building Code of Canada (2020) 15th ed. Canadian Commission on Building and Fire Codes and National Research Council of Canada, Ottawa, ON, 2022.

Seed, H. Bolton, and I. M. Idriss. (1971). Simplified procedure for evaluating soil liquefaction potential. *Journal of the Soil Mechanics and Foundations*[1] *Division, ASCE*, *97*(SM9), 1249-1273.

Seed, H. Bolton, and I. M. Idriss. (1970). *Soil Moduli and Damping Factors for Dynamic Response Analyses*. Report No. EERC 70-10, Earthquake Engineering Research Center, University of California, Berkeley.

Wang, J.-N. (1993). *Seismic Design of Tunnels: A Simple State-of-the-Art Design Approach*. Parsons Brinckerhoff, Inc.